

AD-A088 515

WASHINGTON UNIV SEATTLE DEPT OF AERONAUTICS AND AST--ETC F/G 13/5
A VOID GROWTH FAILURE CRITERION APPLIED TO DYNAMICALLY AND STAT--ETC(U)
JUN 80 A M RAYENDRAN, I M FYFE DAAG29-77-6-0211

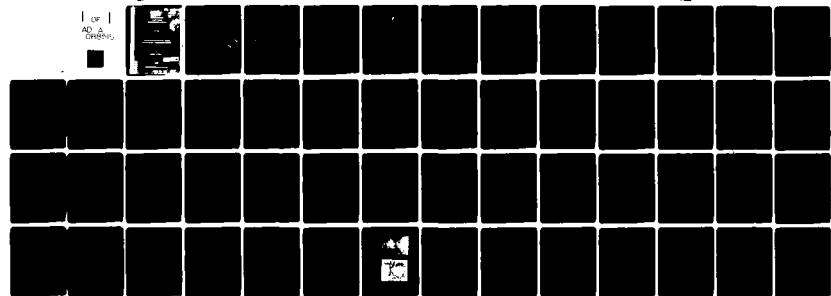
UNCLASSIFIED

80-10

ARO-15078.1-E

NL

1 OF 1
AD-A088 515



END
DATE
FILED
9-80
1 DTIC

6 A VOID GROWTH FAILURE CRITERION APPLIED TO
DYNAMICALLY AND STATICALLY LOADED THIN RINGS.

9 TECHNICAL REPORT

10 A. M. / RAJENDRAN ■ I. M. / FYFE

12 55

11 JUN 1980

14 89-1P

U. S. ARMY RESEARCH OFFICE

15 DAAG 29-77-G-0211



DEPARTMENT OF AERONAUTICS AND ASTRONAUTICS
UNIVERSITY OF WASHINGTON
SEATTLE, WASHINGTON

APPROVED FOR PUBLIC RELEASE;
DISTRIBUTION UNLIMITED.

370273 mt

THE FINDINGS IN THIS REPORT ARE NOT TO BE
CONSTRUED AS AN OFFICIAL DEPARTMENT OF
THE ARMY POSITION, UNLESS SO DESIGNATED
BY OTHER AUTHORIZED DOCUMENTS.



ABSTRACT

The introduction of inertia terms in the theoretical model of thin ring expansion shows that classical plastic instability concepts, defined in terms of the local strain in the necking region, no longer apply. However, in this report it is shown that, when the plastically incompressible constitutive model is replaced with a model applicable to porous plastic materials, a criterion based on critical void volume fraction provides an alternative means to predict failure. The theory also provides a method in which both geometric and metallurgical imperfections in a given sample might be considered. The application of this theory to thin ring specimens was used to confirm that the critical void growth concept predicts the uniform strain at failure as observed in aluminum and copper rings, under both quasi-static and high strain-rate loading conditions.

Accession No.	
NTIS GRAAI	
DDC TAB	
Unnumbered	
Justification	
By	
Distribution	
Availability Terms	
Dist.	Available or Special

P1

CONTENTS

	Page
ABSTRACT	ii
LIST OF ILLUSTRATIONS	iv
1. INTRODUCTION	1
2. PLASTIC INSTABILITY OF INCOMPRESSIBLE MATERIALS	6
2.1 Inertia Effects	6
2.2 Constitutive Models	11
2.3 Strain-Rate Sensitivity and Strain Hardening	14
3. VOID GROWTH FAILURE ANALYSIS	19
3.1 Constitutive Relations for a Compressible Material . .	19
3.2 Dynamic and Static Models	22
3.3 Critical Void Growth	26
4. EXPERIMENTAL VERIFICATION	32
4.1 Dynamic Tests	32
4.2 Static Tests	37
4.3 Experimental Results	38
5. CONCLUSIONS	42
REFERENCES	44

LIST OF ILLUSTRATIONS

Figure	Page
1 The Influence of Strain-Rate on the Imperfection Growth for a Rate-Independent Material ($\sigma = K\epsilon^n$).	10
2 The Influence of Strain-Rate on the Imperfection Growth for a Rate-Dependent Material	13
3 Effect of Strain-Rate Sensitivity on Imperfection Growth Under Static and Dynamic Loading	15
4 Effect of Strain Hardening on Imperfection Growth Under Static and Dynamic Loading	16
5 Imperfection Growth for Non-zero Deceleration of the Uniform Segment	18
6 Imperfection Growth as a Function of Uniform Strain for Different Geometric Imperfection Levels (a) Local Strain, (b) Void Growth ($\Delta f = 0.01$, $n = 0.05$).	27
7 Imperfection Growth as a Function of Uniform Strain for Different Metallurgical Imperfection Levels (a) Local Strain, (b) Void Growth ($n = 0.01$, $n = 0.05$)	28
8 Critical Void Volume Criterion Applied to Thin Rings of Aluminum and Copper	31
9 Specimen Configuration: dynamic (a), static (b)	33
10 Schematic of Photomultiplier Strain-Rate Detector	35
11 Expanded Ring Specimens (a), Typical SEM of Fracture Surface (b)	41

1. INTRODUCTION

Ductile failure as a phenomenon associated with plastic instability dates back to the time of Considère (1885) who identified the point of instability as the onset of localized necking brought about when the increment of strain hardening became equal to the geometric softening, at the point of maximum load in a simple tension test. Marciniaik and Kuczynski (1967) considered this phenomenon in metal sheets under biaxial tension, and developed a mathematical model (M-K model) to construct forming limit diagrams. This model is based on an initial geometric imperfection, which is a localized thickness reduction in the sheet lying perpendicular to the major principal strain direction. By this method they predicted that the local strain in the defective region would grow asymptotically with respect to the strain in the uniform region. Later, Marciniaik, Kuczynski and Pokova (1973) extended this methods to include the influence of the material strain-rate sensitivity on necking behavior under biaxial tension, and concluded that the value of the limit-strain in a forming limit diagram would increase even for very low values of strain-rate sensitivity. In recent studies by Hutchinson and Neale (1977) and Ghosh (1977) the analysis was extended to include the effect of strain-rate and different viscoplastic constitutive laws on localized necking. The results of this analysis, in its application to the case of uniaxial tension under quasi-static loading, also predicted that the strain at necking increases with an increase in the strain-rate sensitivity and the strain hardening parameter. These results were verified experimentally for different materials by Ghosh (1977). The above analysis

also predicted, depending upon the constitutive equation, either no effect on or minor reduction of uniform strain at necking due to an increase in strain-rate. These theoretical results were in agreement with the experiments of Sagat and Taplin (1976) for superplastic materials under quasi-static loading conditions.

In the high strain-rate loading regime, where the quasi-static loading assumption no longer applies, considerable evidence exists, Wilson (1964), that an increase in strain-rate can in fact result in an increase in the ductility of most metals. In a series of experiments at high strain-rate the present authors (Fyfe and Rajendran, 1980) confirmed the increased ductility which occurs in this regime. They also supported this evidence by applying the M-K model to thin ring failure when inertia effects were included. Interestingly the numerical solution of this model predicted the expected slow-down in the imperfection growth rate, but, in this case, even though the local strain grows faster than the uniform strain, no plastic instability condition occurs before the material has actually failed. Physically it is rational to expect the uniform strain to grow continuously with the local strain due to inertia; so, the developed stability model for ring specimen does not provide an inherent failure or flow localization criterion under dynamic loading condition. In this case, additional information or some other method has to be considered to predict failure. One way is to postulate that failure will occur when some macro/micro parameter reaches a finite critical value. For this purpose, it is essential to consider the failure mechanism at the local site where the failure would eventually occur.

A failure mechanism with growing acceptability, is one which considers the process as being initiated by the nucleation of voids around inclusions and their subsequent growth and coalescence as suggested by McClintock (1968). During the last decade, different approaches were initiated by several investigators to apply this mechanism as a means of predicting ductile failure. Among them, Rice and Tracey (1969) considered the growth kinetics of a single void in the matrix and developed a model which showed the dependence of void growth rate on the triaxiality of the stress state. Hancock and MacKenzie (1975) provided the experimental evidence to support this dependency on stress state and used this model to predict failure initiation in an approximate manner.

Seaman, Barbee and Curran (1971) earlier developed empirical criteria to predict the nucleation and growth rates of voids under dynamic loading condition and developed extensive computer codes to predict failure.

Metallurgical evidence in support of the void growth mechanism has also been developed (Gurland and Plateau (1963), Beachem (1963), Darlington (1971), Argon, Im and Safoglu (1975)) where fractured specimens were examined to provide the metallographic data required.

Encouraged by the physical evidences, several other investigators (Berg, 1969, Nagpal, et al., 1972) working on the continuum aspect of failure, considered plastic dilatation effects on the yield criterion. This gave a new dimension to the problem of ductile fracture. Following this line of attack, recently Gurson (1975) presented a continuum theory of ductile rupture by void nucleation and growth and he came up with a constitutive equation for void-containing materials, which explicitly considered the void volume fraction and matrix stresses. The main

advantage of such a theory is its simplicity and its ability to provide direct calculations of these micro-parameters which are essential to predict failure.

This continuum model was employed by Yamamoto (1977) in a study of shearband localization in porous materials. In this study, the initial metallurgical imperfection is described by stipulating a slightly larger value for the void volume fraction in the local site compared to that in the uniform region; whereas Needleman and Triantafyllidis (1979) considered both geometric and metallurgical imperfections in their study, using Gurson's constitutive equation to predict forming limit diagrams, and concluded that their theoretical results were in agreement with the available experiments.

The work described in this report is presented in two parts. The first follows the pattern established by earlier investigators by examining the role played by strain-rate sensitivity and the strain-hardening parameters on the kinetics of imperfection growth under dynamic loading conditions, particularly as they are influenced by the various viscoplastic constitutive models. In this portion of the study the material is assumed to be plastically incompressible, and no attempt is made to incorporate a failure criterion to replace the plastic instability condition found in quasi-static failure. The second part is directly applied to examining the failure levels as they occur under both static and dynamic conditions, using the constitutive model proposed by Gurson in conjunction with M-K methods. Imperfections of both metallurgical and geometric origins in ring specimens are considered. Based on metallographical observations on the fractured ring specimens, it was postulated that under dynamic

loading condition the failure would occur when the void volume fraction reached a critical value which could be obtained from the solution of the quasi-static stability model for a plastic compressible material. The validity of such a criterion was verified by comparing the theoretical and experimental values of the uniform strain under both static and dynamic loading conditions.

2. PLASTIC INSTABILITY OF INCOMPRESSIBLE MATERIALS

For rate-independent materials a simple stability criterion can be readily derived from Considères model of plastic instability. This model predicts the onset of necking at a strain value of $\epsilon = n$ in a tensile test specimen, when the power law, $\sigma = K\epsilon^n$, is used, where n is the strain hardening parameter, K is the strength coefficient, σ is the uniaxial stress and ϵ is the strain. However, in the case of rate dependent materials, several authors (Hart, 1967; Campbell, 1967; Jonas et al., 1977; Demeri and Conrad, 1978) developed stability models which allowed for strain-rate sensitivity. Unfortunately a number of conflicting results arose from these studies, which were only recently resolved in a comprehensive study reported by Ghosh (1977), who examined plastic instability and necking in materials with strain and strain-rate hardening. The above studies were all quasi-static in nature, and hence no inference can be drawn as to what effects inertia might have on the process. This effect can best be examined from both an experimental and theoretical point-of-view, by considering the expansion of thin rings under impact loading, rather than the tensile bar configuration most commonly considered in the previously cited studies.

2.1 Inertia Effects

The nonlinear long-wavelength analysis of Hutchinson and Neale (1977) can be adapted to include inertia, by examining the radial symmetric expansion of a thin ring or cylinder. The hoop strain (ϵ) and the radial strain (ϵ_r) can be described in terms of radial displacement (u) by

$$\epsilon = \ln\left(\frac{r}{R}\right) = \ln(1 + u/R), \quad \epsilon_r = \ln \frac{h(t)}{h(0)} \quad (2.1)$$

where R is the initial radius of the mid-surface, $r(t)$ is the instantaneous radius, with $h(0)$ the initial thickness and $h(t)$ the instantaneous thickness. If we assume the material is plastically incompressible ($\epsilon + \epsilon_r + \epsilon_z = 0$), and that the only significant stress is the hoop stress, then we obtain the relationship between ϵ_r and ϵ , which has the form

$$\epsilon_r = \epsilon_z = -\epsilon/2. \quad (2.2)$$

From (2.1) and (2.2) we can now obtain the relation

$$h(t) = h(0)e^{-\epsilon(t)/2}. \quad (2.3)$$

Consider two segments of the expanding thin strip or ring, one with a small defect in the thickness, and the other with uniform thickness. The variables associated with these two segments can be distinguished by using the subscript "0" for the uniform segment, and so we can let n define a non-uniformity parameter

$$n = \frac{h_0(0) - h(0)}{h_0(0)} \quad (2.4)$$

By combining (2.3) and (2.4) we can obtain an expression relating the change in thickness of the uniform and local segments to the hoop strain of the form

$$\frac{h_0(t)}{h(t)} = \frac{1}{1-n} e^{(\epsilon-\epsilon_0)/2}. \quad (2.5)$$

The equation of motion for an expanding ring for a given internal pressure $P(t)$ is, for the uniform section,

$$P(t) = \frac{\sigma_0 h_0}{r_0} + \rho h_0 \ddot{u}_0 \quad (2.6)$$

for the local section

$$P(t) = \frac{\sigma h}{r} + \rho h \ddot{u} \quad (2.7)$$

where σ is the hoop stress, ρ is the mass density, r is the instantaneous radius, and \ddot{u} is the radial acceleration of the ring. Since the pressure experienced by both segments is the same we can equate (2.6) and (2.7) to obtain

$$\frac{\sigma h}{r} + \rho h \ddot{u} = \frac{\sigma_0 h_0}{r_0} + \rho h_0 \ddot{u}_0. \quad (2.8)$$

From (2.1) we can obtain \ddot{u} and r in terms of the hoop strain so that (2.8) has the form

$$\ddot{\epsilon} + \dot{\epsilon}^2 = \frac{e^{-(\epsilon + 3\epsilon_0)/2}}{(1 - n)\rho R^2} (\sigma_0 + \rho R^2 e^{2\epsilon_0} (\ddot{\epsilon}_0 + \dot{\epsilon}_0^2)) - \frac{e^{-2\epsilon}}{\rho R^2} \sigma. \quad (2.9)$$

Before examining the dynamics failure process the quasi-static case can also be considered by neglecting the inertia terms as represented by the strain-rate terms in Equation (2.9). If the material is assumed to obey the rate independent power law, $\sigma = K\epsilon^n$, Equation (2.9) reduces to the form

$$\dot{\epsilon}^n = \frac{e^{3/2(\epsilon - \epsilon_0)}}{(1 - n)} \epsilon_0^n.$$

Using the failure criterion, $d\epsilon/d\epsilon_0 \rightarrow \infty$, as proposed by Hutchinson and Neale (1977), it can readily be determined that the onset of local necking occurs when $\epsilon = \frac{2}{3}n$, which is compatible with the tension bar results of $\epsilon = n$. The corresponding value of the uniform strain ϵ_0^c at that point

will obviously be less than $\frac{2}{3}n$ and the value can be obtained by the numerical solution of the following transcendental equation for a given value of n .

$$\frac{3\epsilon_0^c}{2n} e^{(1 - \frac{3\epsilon_0}{2n})} = (1 - n)^{1/n} \quad (2.11)$$

When there is no geometric imperfection, $n = 0$, the classical result of Considére, $\epsilon_0 = \frac{2}{3}n$ is obtained directly from Equation (2.11).

The material response of the ring when it expands under dynamic loading conditions can be obtained from the numerical solution of Equation (2.9), where again the power law applies, and the uniform strain-rate is obtained from the derivative of Equation (2.1), which can be written as

$$\dot{\epsilon}_0(t) = \frac{\dot{u}_0}{R} e^{-\epsilon_0} \quad (2.12)$$

For reasons of simplicity it has been assumed that the ring is expanding at a constant velocity, and so Equation (2.9) is simplified in that $(\ddot{\epsilon}_0 + \dot{\epsilon}_0^2)$ is zero. The constant velocity of the expanding ring is defined through the initial uniform strain rate $\dot{\epsilon}_0$. In Figure 1, curves of the local strain ϵ are plotted against the uniform strain ϵ_0 for different initial strain-rate values. These plots clearly show the growth of the local strain is inhibited by increasing strain rate, which is in accord with experimental observations. These results also show that the quasi-static failure criterion $d\epsilon/d\epsilon_0 \rightarrow \infty$ is no longer applicable, and some other failure criterion must be introduced. The results presented in Figure 1 are based on the assumption that the material is strain-rate independent. However, as was pointed out earlier, the material

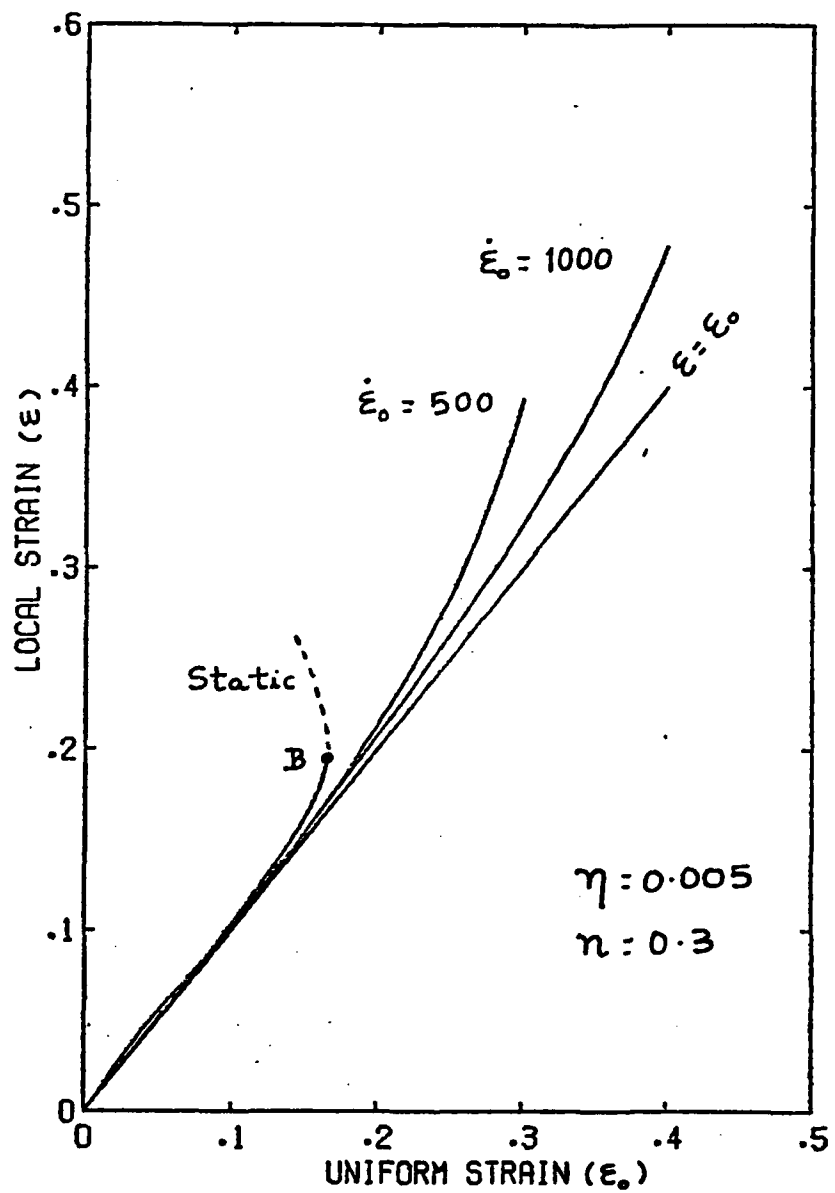


Fig. 1 The Influence of Strain-Rate on the Imperfection Growth for a Rate-Independent Material ($\sigma = K\epsilon^n$).
B point of static load maximum (Considére's criterion).

strain-rate sensitivity is an important parameter in the failure process. In the high strain-rate regime considered in this investigation the power law constitutive model may no longer be applicable and more complex models must be considered.

2.2 Constitutive Models

The sensitivity of materials to strain-rate has been extensively studied as it relates both to creep behavior and high rates of loading. In considering ductile fracture, strain-rate sensitivity has usually been associated with the creep regime. However, when high strain-rate regimes are included a much wider range of constitutive models are available for consideration. It is thus necessary to determine how important the choice of a constitutive model is in the calculation of the local strain growth. For this purpose three different additive types of viscoplastic uniaxial constitutive equations are introduced into the basic failure Equation (2.9). These constitutive models, discussed quite extensively in the literature, have the form

$$\sigma = K(\epsilon^n + m \ln(\dot{\epsilon}/\dot{\epsilon}_{ref})) \quad (2.13)$$

$$\sigma = K\epsilon^n(1 + m \ln(1 + \dot{\epsilon}/\dot{\epsilon}_{ref})) \quad (2.14)$$

and

$$\sigma = K(\epsilon^n + m' \ln(1 + \frac{\sqrt{3}}{2} \frac{\dot{\epsilon}}{\dot{\epsilon}_{ref}})) \quad (2.15)$$

where $\dot{\epsilon}_{ref}$ is the reference strain-rate below which the material is considered to be strain-rate insensitive, and m is a strain-rate sensitivity parameter.

The constitutive law (2.13) is a particular form of the equation proposed by Deutler (1932) and is used by Ghosh (1976) and Hutchinson and

Neale (1977) in their analyses of necking under uniaxial tension. This model was essentially derived for materials having low $\dot{\epsilon}_{ref}$ in the quasi-static loading regime. The constitutive Equation (2.14) is the one proposed by Campbell, et al. (1976), for copper and it was experimentally evaluated for strain-rate levels covering both quasi-static and dynamic loading regimes ($\dot{\epsilon} = 10^{-6}$ to 10^3 sec $^{-1}$). This model is a modified version of the Malvern overstress equation (1951). The last equation is basically a one-dimensional version of a Perzyna (1966) type viscoplastic model which has been extensively used in the analysis of plastic stress wave propagation. All three of the above equations were considered as being applicable to materials with low strain-rate sensitivity ($m \leq 0.06$). For instance the materials tested by Ghosh (1977b) in his study of post-uniform elongation in a uniaxial tensile test of a thin strip, fall in this range of m .

The numerical solution of Equation (2.9) with any of the above constitutive models gives results which are very similar to those shown in Figure 1. In particular, for the high strain-rate condition the growth of the local strain relative to the uniform strain is essentially identical for all three models. This feature can be readily seen from the results of this analysis as presented in Figure 2. It thus can be concluded that the inclusion of inertia terms in the analysis leads to a deformation process in which the choice of a constitutive model is, within reason, not a particularly critical one. At low strain-rate values, where the inertia terms might reasonably be ignored, the models do predict different levels of uniform strain that can be reached before significant

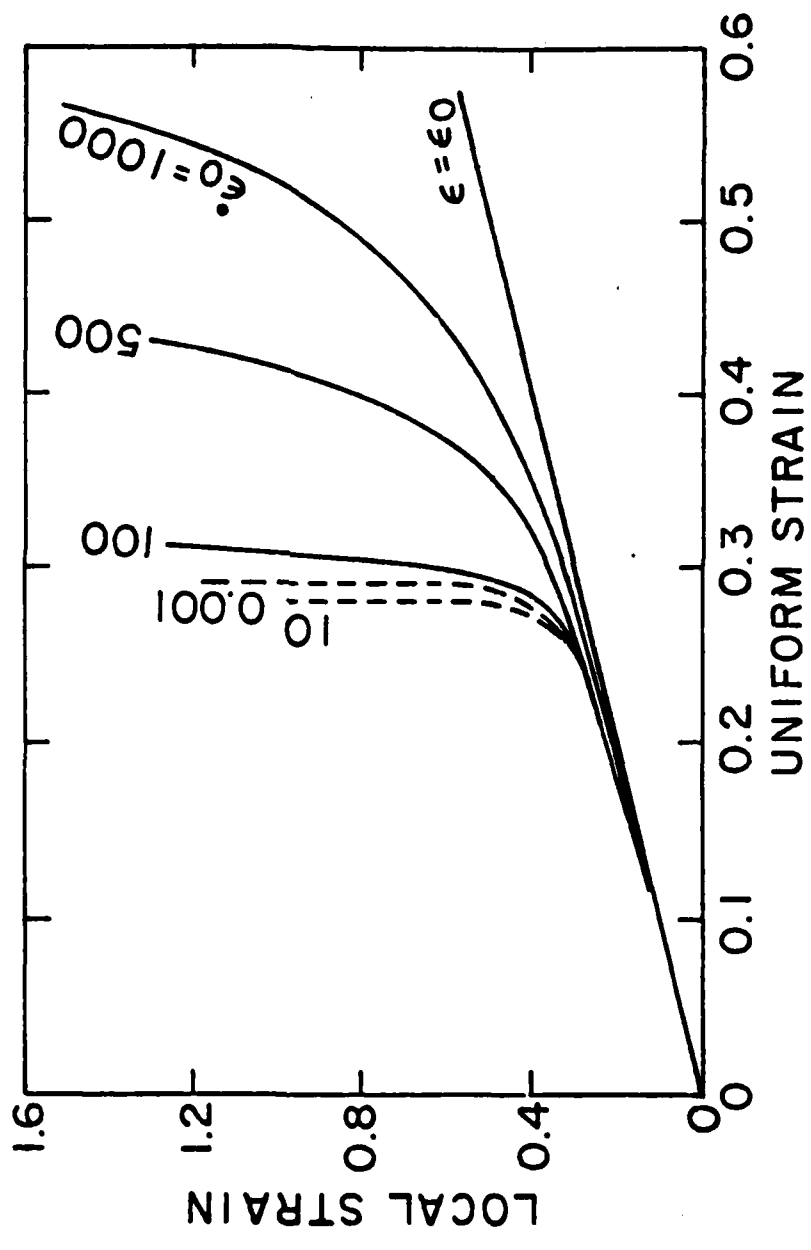


Fig. 2 The Influence of Strain-Rate on the Imperfection Growth for a Rate-Dependent Material. --- without inertia, — with inertia.

necking occurs. The curves of Figure 2 indicate that necking occurs earlier for an increased in strain-rate for the model of Equation (2.14). This is also the case for the model of Equation (2.13) as was reported by Hutchinson and Neale (1977). On the other hand the Perzyna model shows only a delay in necking with increased strain rate.

However, all models show a delay in necking if the inertia is included regardless of the strain-rate level. Unfortunately the change in the value of the uniform strain at these low strain-rate levels is not very large, and the limited experimental evidence available to check this particular feature precludes its use as a means of determining the most suitable constitutive model to use in ductile fracture studies.

Although inertia terms dominate the failure process it does not eliminate the importance of strain-rate sensitivity or strain-hardening, and these two properties are examined in the following section.

2.3 Strain-Rate Sensitivity and Strain Hardening

The strain-hardening parameter n and the strain-rate sensitivity parameter m are contained in all three constitutive models introduced in the previous section. As these constitutive models predict essentially the same variation of imperfection growth to changes in n or m , it is sufficient to demonstrate their influence to dynamic loading conditions by reporting the results obtained using Equation (2.14).

The variation of the local strain as a function of increasing uniform strain is shown in Figures 3 and 4 for various values of n and m . From these curves it can be seen that when the inertia terms are low, or omitted from the calculations, the imperfection growth is quite sensitive

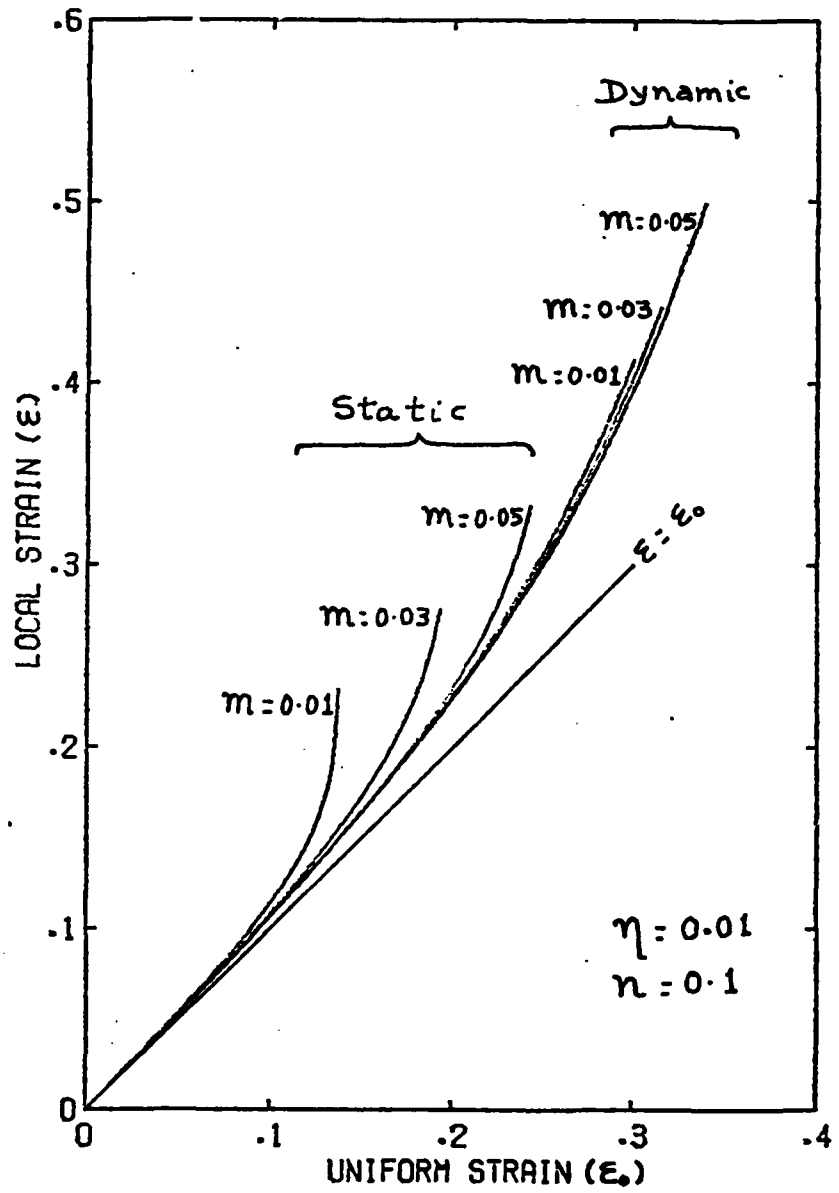


Fig. 3 Effect of Strain-Rate Sensitivity on Imperfection Growth Under Static and Dynamic Loading.

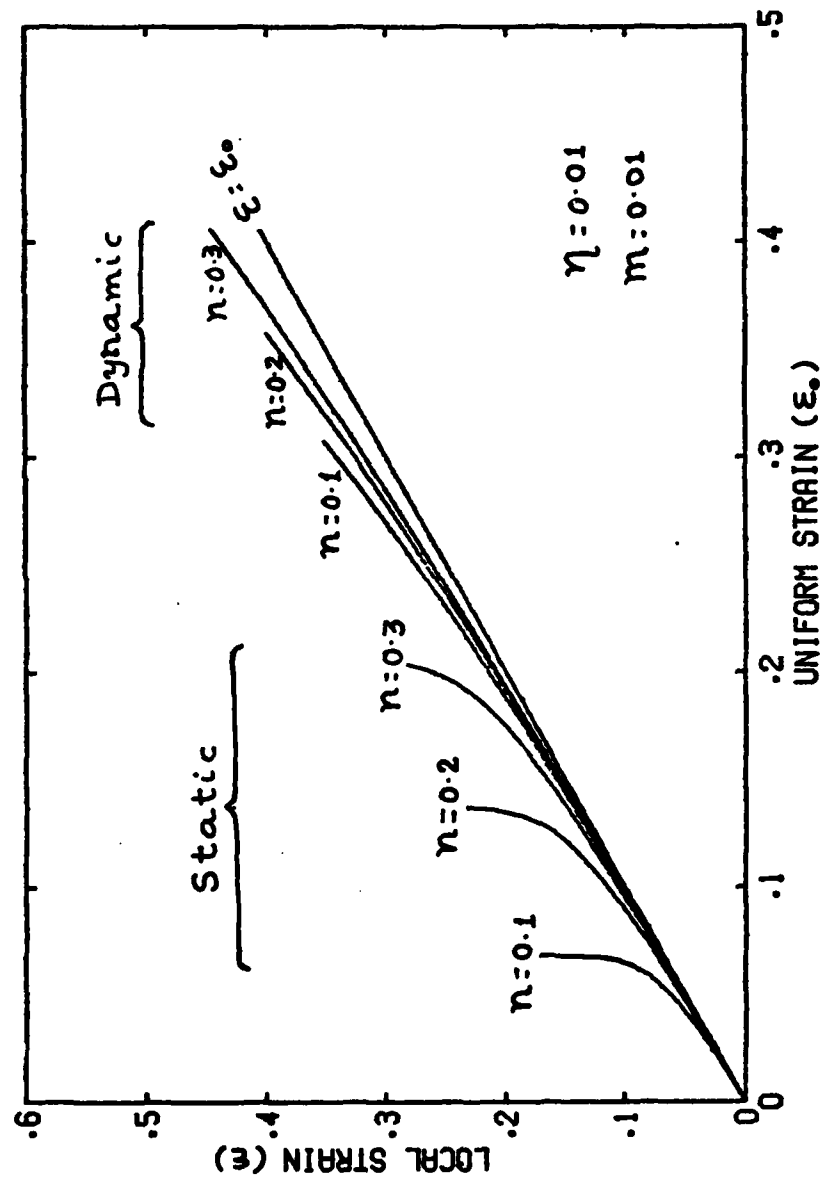


Fig. 4 Effect of Strain Hardening on Imperfection Growth Under Static and Dynamic Loading.

to the value chosen for these parameters. Also, as is to be expected from the results of other investigations, increasing the strain hardening or strain-rate sensitivity increases the value of the uniform strain at which significant necking might be expected to occur.

It is interesting to note that at the higher strain-rate levels the variation in the curves, due either to different values of n or m or the strain rate, becomes less significant as the process approaches the limiting curve $\epsilon = \epsilon_0$. This feature allows a greater degree of flexibility in carrying out high strain-rate tests, in that the strain-rate levels need not be defined so precisely. However, it also limits using this type of test as a means of determining material parameters.

If the assumption that the ring is expanding at a constant velocity is replaced by the more general case in which the ring is expanding with a constant deceleration of the uniform segment, then the solution of Equation (2.9) gives the results shown in Figure 5. As one would expect when the inertia level rapidly decreases the imperfection grows faster relative to the uniform strain than for the constant velocity case. This, of course, indicates that to obtain the maximum deformation before failure the strain-rate must remain high throughout the complete deformation. The trend of these results were qualitatively the same for both the power law and visco-plastic constitutive models.

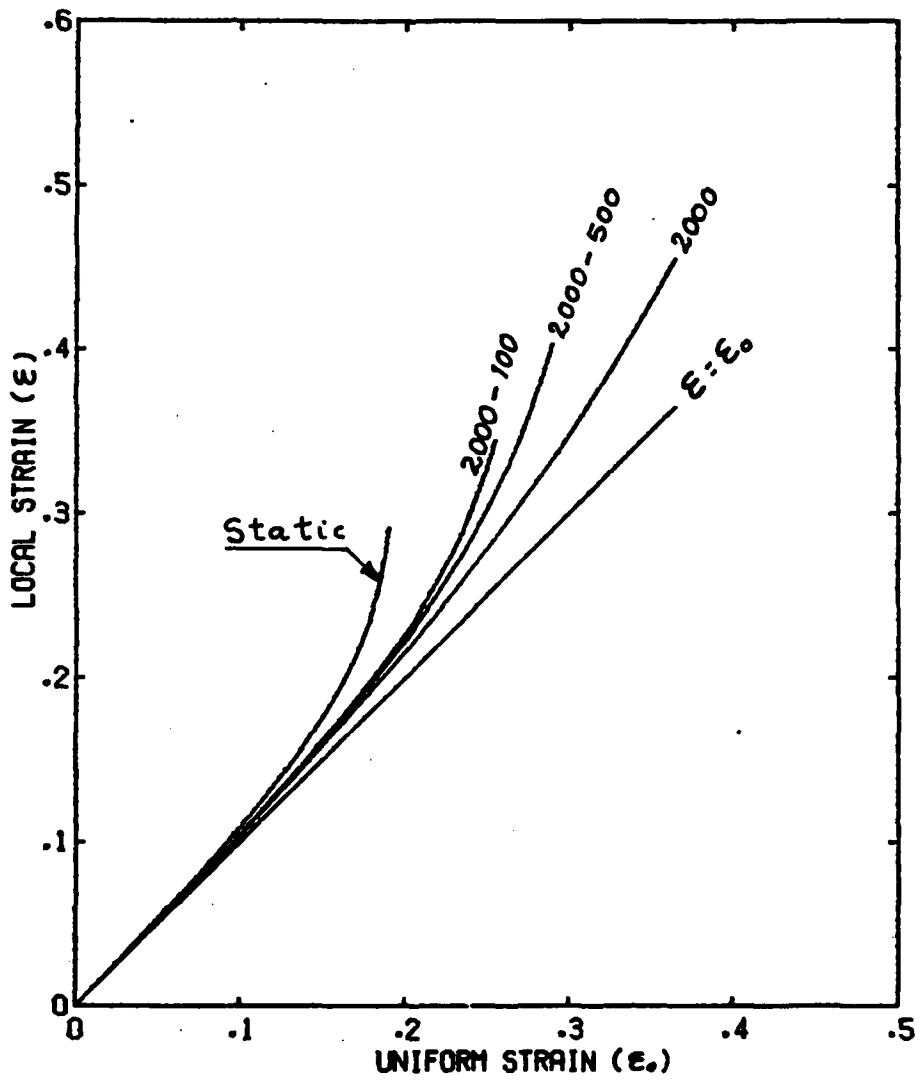


Fig. 5 Imperfection Growth for Non-zero Deceleration of the Uniform Segment. ($\dot{\epsilon}_0 = 2000 \text{ 1/sec}$).

3. VOID GROWTH FAILURE ANALYSIS

Although the stability model for a plastically incompressible material provides the theoretical confirmation that plastic instability is inhibited due to inertia effects, it does not contain an inherent criterion for localized necking or failure. The failure criterion $d\epsilon/d\epsilon_0 \rightarrow \infty$ used in Section 2.1 must therefore be replaced if failure under high strain-rate conditions is to be predicted.

In recent years both experimental and theoretical studies of ductile failure have provided sufficiently strong evidence to suggest that the growth of voids is an important mechanism in the process. This type of behavior is usually associated with high "tri-axiality" stress conditions, but it has been used at relatively low mean stress levels by Hancock and Mackenzie (1976) in their analysis of notched tensile specimens.

In this section the failure process will be considered assuming that the presence of voids will require that the material be plastically compressible. Following an approach used by Needleman and Triantafyllidis (1978), the material will be described using the constitutive model proposed by Gurson (1975). By this means it is possible to combine both geometric and metallurgical imperfections in the analysis.

3.1 Constitutive Relations for a Compressible Material

The constitutive relations used in this study very closely follows the form used by Needleman and Triantafyllidis (1978) and for this reason details of the derivation of these equations are omitted. However, for completeness, and also to show how the equations are adapted to the

geometry and strain-rate conditions appropriate to dynamically loaded thin ring specimens, the necessary equations are presented in this section. For a randomly voided material the yield surface has the form

$$\phi = \frac{\sigma_e^2}{Y_m^2} + 2fcosh\left(\frac{\sigma_1 + \sigma_2 + \sigma_3}{2Y_m}\right) - f^2 - 1 = 0 \quad (3.1)$$

where Y_m is the flow stress of the matrix material, f is the current volume fraction of voids, σ_i are the principle values of the Cauchy stress acting on an element of the void matrix aggregate and σ_e is the effective stress.

The increment in Y_m has the form

$$\dot{Y}_m = \frac{E_t E}{(E - E_t)Y_m} \cdot \frac{\sigma_i \dot{\epsilon}_i^p}{(1 - f)} \quad (3.2)$$

where E and E_t are the Young's modulus and tangent modulus respectively of the incompressible matrix. It is through E_t that the constitutive relations of the type described by Equations (2.13), (2.14) and (2.15) are introduced into the analysis. The rate of change of the void volume fraction f , and the plastic dilation are related by

$$\dot{f} = (1 - f)(\dot{\epsilon}_1^p + \dot{\epsilon}_2^p + \dot{\epsilon}_3^p) \quad (3.3)$$

while the plastic strain rate $\dot{\epsilon}_i^p$ of the aggregate is given by

$$\dot{\epsilon}_i^p = \frac{1}{g} \frac{\partial \phi}{\partial \sigma_k} \cdot \dot{\sigma}_k \frac{\partial \phi}{\partial \sigma_i} \quad (3.4)$$

with

$$g = - \left| \frac{\partial \phi}{\partial Y_m} \cdot \frac{E_t E}{E - E_t} \cdot \frac{\sigma_i}{(1-f)Y_m} \cdot \frac{\partial \phi}{\partial \sigma_i} \right. \\ \left. + \frac{3f(1-f)}{Y_m} \frac{\partial \phi}{\partial f} \sinh\left(\frac{\sigma_1 + \sigma_2 + \sigma_3}{2Y_m}\right) \right| \quad (3.5)$$

Following the approach taken by Needleman and Triantafyllidis (1978) the constitutive equation of the principal stress components of the aggregate can be written in the following fashion

$$\dot{\sigma}_i = C_{ij} \dot{\epsilon}_j \quad (3.6)$$

where it has been assumed that the total strain rate is the sum of its elastic and plastic increments. Thus Equation (3.4) can be combined with the elastic stress-strain relations so that the coefficients C_{ij} are given by,

$$C_{ij} = E_{ij} - \frac{1}{q} E_{ik} \frac{\partial \phi}{\partial \sigma_k} E_{ij} \frac{\partial \phi}{\partial \sigma_i} \quad (3.7)$$

where

$$q = g + \frac{\partial \phi}{\partial \sigma_i} E_{ij} \frac{\partial \phi}{\partial \sigma_j} \quad (3.8)$$

and the elastic constants of the matrix are given in terms of Young's modulus E , and Poisson's ratio ν , by

$$E_{ij} = \begin{cases} \frac{E(1-\nu)}{(1+\nu)(1-2\nu)} & i = j \\ \frac{\nu E}{(1+\nu)(1-2\nu)} & i \neq j \end{cases} \quad (3.9)$$

The above equations thus describe the compressible material in the necking region. For a plane stress problem these equations can be greatly reduced in complexity, so that the plane stress increments are given by

$$\dot{\sigma}_{\alpha} = L_{\alpha\beta} \dot{\epsilon}_{\beta} \quad (3.10)$$

where the plane stress moduli $L_{\alpha\beta}$ are related to the C_{ij} coefficients by the expressions

$$L_{\alpha\beta} = C_{\alpha\beta} - \frac{C_{az} C_{z\beta}}{C_{zz}} \quad (3.11)$$

in which the Greek indices range from 1 to 2 in contrast to the Latin indices which range from 1 to 3. Equation (3.11) can be further reduced for the uniaxial stress case where Equation (3.10) will then have the form

$$\dot{\sigma} = (L_{11} - \frac{L_{12}L_{21}}{L_{22}})\dot{\epsilon} \quad (3.12)$$

The constitutive equations of the compressible material as described by either Equations (3.6), (3.10) or (3.12) do not explicitly contain the strain-hardening or strain-rate sensitivity parameters n and m . These parameters, as was mentioned earlier, enter the problem through the description of the material matrix as represented by Y_m or more specifically E_t .

With the above background on the constitutive relationships for compressible material the application of these equations to failure under either quasi-static or dynamic loading can now be considered for the thin ring configuration.

3.2 Dynamic and Static Models

As in the earlier analysis the hoop strain (ϵ_θ) and the radial strain (ϵ_r) can be described by Equations (2.1). However, with the assumption of plastic incompressibility no longer applied, these two strains are no longer directly related, so that the instantaneous thickness and radius are now given by

$$h(t) = h(0)e^{\epsilon_r}, \quad r(t) = R e^{\epsilon_\theta} \quad (3.13)$$

To distinguish between the variables as they apply to either the uniform or local segments of the ring the superscripts "u" and "l" are introduced

compressible material case. The initial geometric imperfection η of Equation (2.4) now has the form

$$\eta = 1 - \frac{h^l(0)}{h^u(0)} \quad (3.14)$$

The equation of motion for the two segments are for the uniform section

$$P(t) = \frac{\sigma_\theta^l h^l}{r^l} + \rho h^l \ddot{u}^l \quad (3.15)$$

and the local section

$$P(t) = \frac{\sigma_\theta^u h^u}{r^u} + \rho h^u \ddot{u}^u \quad (3.16)$$

As for the compressible case we can eliminate the pressure $P(t)$ by equating Equations (3.15) and (3.16) to obtain

$$\ddot{\epsilon}_\theta^l + (\dot{\epsilon}_\theta^l)^2 = \frac{\sigma_\theta^u}{\rho R^2(1-\eta)} \cdot e^{-(\epsilon_\theta^l + \epsilon_\theta^u)} \cdot e^{(\epsilon_r^u - \epsilon_r^l)} - \frac{\sigma_\theta^l e^{-2\epsilon_\theta^l}}{\rho R^2} \quad (3.17)$$

where Equations (3.13) and (3.14) have been used to express \ddot{u} , h , and r in terms of the strains ϵ_θ , ϵ_r , and the imperfection η . Again for reasons of simplicity it has been assumed that the ring is expanding at a constant velocity ($\dot{u}^u = 0$).

If the material is assumed to be incompressible then the plastic incompressibility condition can be used to reduce the above equation to the earlier form as described by Equation (2.9).

Before examining the dynamic failure process the quasi-static case can also be considered by neglecting the inertia terms as represented by the strain-rate terms in Equation (3.17) and so this equation is reduced to the form

$$\sigma_\theta^L e^{(\epsilon_r^L + \epsilon_\theta^U)} = \frac{1}{(1-\eta)} \sigma_\theta^U e^{(\epsilon_r^U + \epsilon_\theta^L)} \quad (3.18)$$

Now, take the time derivative of the above in order to introduce the stress-strain relation (3.10) and the Equation (3.18) becomes,

$$\dot{\sigma}_\theta^L + \sigma_\theta^L (\dot{\epsilon}_r^L + \dot{\epsilon}_\theta^U) = F(\dot{\sigma}_\theta^U + \sigma_\theta^U (\dot{\epsilon}_r^U + \epsilon_\theta^L)) \quad (3.19)$$

where

$$F = \frac{1}{(1-\eta)} e^{(\epsilon_r^U - \epsilon_r^L)} e^{(\epsilon_\theta^L - \epsilon_\theta^U)} \quad (3.20)$$

Both in the quasi-static and dynamic cases the local and uniform segments were considered to be under plane stress ($\dot{\sigma}_r = 0$) and uniaxial stress conditions respectively. For these stress conditions the following equations are used in the numerical solution for both the static and dynamic cases.

From $\dot{\sigma}_r = 0$ we get

$$\dot{\epsilon}_r = \gamma_\theta \dot{\epsilon}_\theta + \gamma_z \dot{\epsilon}_z \quad (3.21)$$

where

$$\gamma_\theta = -\frac{C_{r\theta}}{C_{rr}} \text{ and } \gamma_z = -\frac{C_{rz}}{C_{rr}} \quad (3.22)$$

Also employing the strain compatibility across the imperfection band, we get

$$\epsilon_z^L = \epsilon_z^U \quad (3.23)$$

Since $\dot{\sigma}_r^U = 0$, the following relation is obtained

$$\dot{\epsilon}_z^U = - \frac{L_{z\theta}^U}{L_{zz}^U} \cdot \dot{\epsilon}_\theta^U \quad (3.24)$$

Using the Equations (3.21) to (3.23) in Equation (3.19), we get

$$(L_{\theta\theta}^\lambda + \sigma_\theta^\lambda \gamma_\theta^\lambda - F\sigma_\theta^U) \dot{\epsilon}_\theta^\lambda = (FL_{\theta\theta}^U + F\sigma_\theta^U \gamma_\theta^U - \sigma_\theta^\lambda) \dot{\epsilon}_\theta^U \\ + (FL_{\theta z}^U + \sigma_\theta^U F\gamma_z^U - L_{\theta z}^\lambda - \sigma_\theta^\lambda \gamma_z^\lambda) \dot{\epsilon}_z^U \quad (3.25)$$

Expressing $\dot{\epsilon}_z^U$ in terms of $\dot{\epsilon}_\theta^U$ through Equation (3.24), the above equations can be modified to the following form

$$\frac{d\epsilon_\theta^\lambda}{d\epsilon_\theta^U} = A \quad (3.26)$$

where

$$A = Q - V \frac{L_{z\theta}^U}{L_{zz}^U}, \quad Q = \frac{FL_{\theta\theta}^U + F\sigma_\theta^U \gamma_\theta^U - \sigma_\theta^\lambda}{L_{\theta\theta}^\lambda + \sigma_\theta^\lambda \gamma_\theta^\lambda - F\sigma_\theta^U}$$

and

$$V = \frac{(FL_{\theta z}^U + F\sigma_\theta^U \gamma_z^U - L_{\theta z}^\lambda - \sigma_\theta^\lambda \gamma_z^\lambda)}{(L_{\theta\theta}^\lambda + \sigma_\theta^\lambda \gamma_\theta^\lambda - F\sigma_\theta^U)} \quad (3.27)$$

The quasi-static instability condition for the compressible material is then defined the same way as it was for the incompressible material, i.e., $d\epsilon_\theta^\lambda/d\epsilon_\theta^U \rightarrow \infty$ or $A \rightarrow \infty$.

The quasi-static and dynamic stability Equations (3.26) and (3.17) can be solved by straight-forward numerical techniques. The variables f , γ_m , σ_i and the strains can be obtained simultaneously for both the segments through the numerical solution of Equations (3.2), (3.3) and

(3.10). The initial metallurgical imperfection (Δf) is defined as the difference between the initial void volume fractions of local and uniform segments. This can be incorporated into the solution by initially setting $f^u = 0$, so that $f^l = \Delta f$.

3.3 Critical Void Growth

The numerical solution of the quasi-static Equation (3.26) was carried out until the necking condition, $A \rightarrow \infty$, was reached. The corresponding values for the uniform strain and the local void volume fraction at this point were described as ϵ_{cr}^s and f_{cr} respectively. The starting point for the computation was the strain at the initial yield of the ring, and the strain increment size was selected so that the yield condition (3.1) and the equilibrium Equation (3.18) were satisfied within a tolerance of 10^{-5} to 10^{-7} . Any further attempt to improve the tolerance level did not produce any change in the results, and so, the optimum step size was used.

The results of these calculations are given in Figs. 6 and 7 for various values of the parameters η and Δf . The sensitivity of the uniform strain at necking to these imperfections can be gauged from these results. For the case where $\eta = 0$ in Fig. 6 and $\Delta f = 0$ in Fig. 7 it can be seen that when either the geometrical or metallurgical imperfection is absent from the specimen local necking can still occur. This means that when the geometric imperfection is either absent or insignificant, as might be the case for a carefully machined notched specimen or a thick plate under impact loading, the metallurgical imperfection alone can trigger the local instability. As a geometric imperfection is always present in a thin specimen, $\eta = 0$ is not considered a valid value for

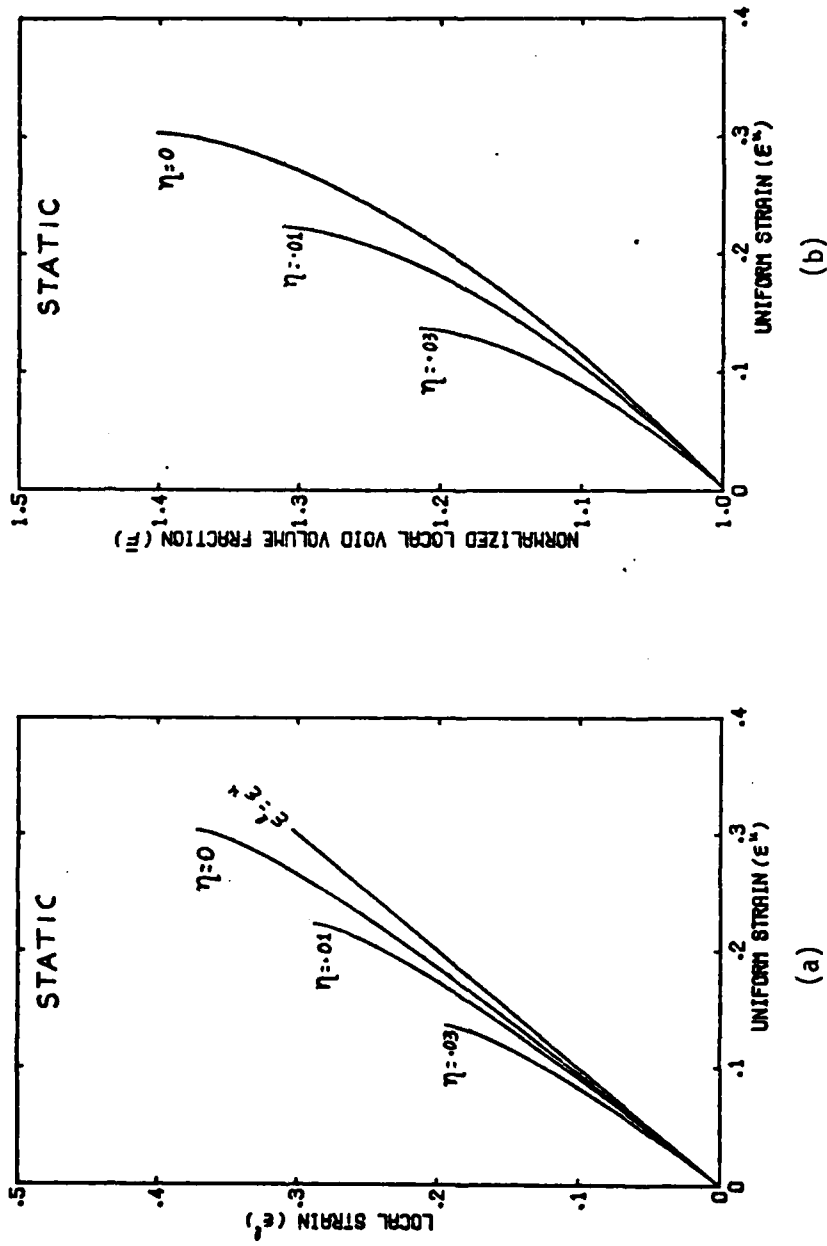
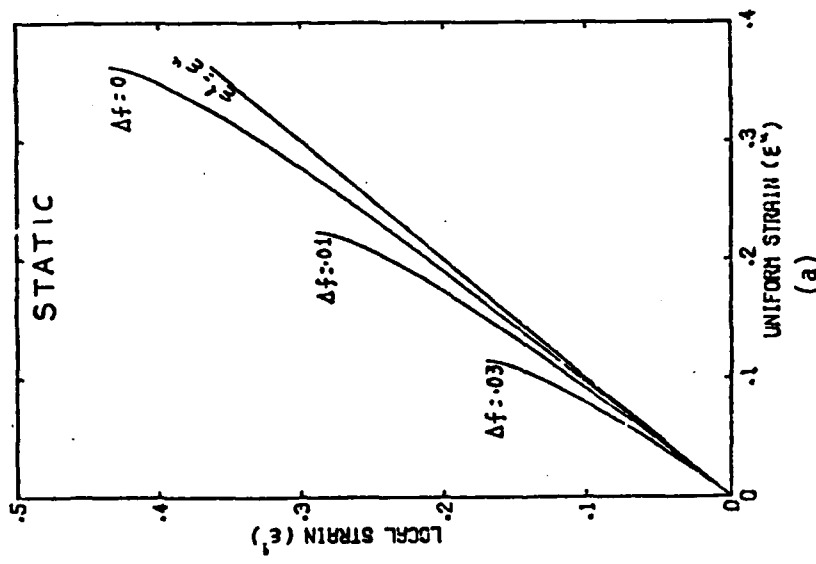
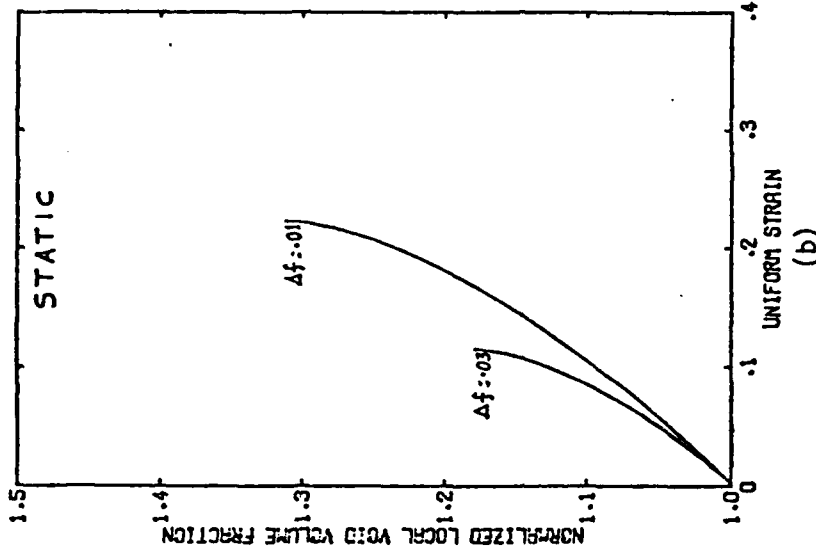


Fig. 6 Imperfection Growth as a Function of Uniform Strain for Different Geometric Imperfection Levels (a) Local Strain, (b) Void Growth ($\Delta f = 0.01$, $n = 0.05$).



(a)



(b)

Fig. 7 Imperfection Growth as a Function of Uniform Strain for Different Metallurgical Imperfection Levels (a) Local Strain, (b) Void Growth ($\eta = 0.01$, $n = 0.05$).

this parameter in these cases.

The dynamic imperfection growth model of Equation (3.17) was solved numerically for various values of the Δf and n parameters. As is to be expected no well defined instability point could be detected. However, these parameters, as in the static case, significantly influence the void growth and local strain, in that strain-rate (or inertia) inhibits the growth of the local strain. From the results shown in Fig. 8 it can be seen that the void growth is also inhibited by the increase in the strain-rate.

With the absence of any well defined point of instability under high strain-rate loading conditions, some alternative failure criterion is required for this case. Two approaches are possible, either to consider a new failure criterion, or find means of extending the quasi-static criterion, $d\varepsilon^u/d\varepsilon^d \rightarrow \infty$, to cover the dynamic case. The latter approach was taken in this study.

Earlier studies by other investigators (Hancock and Mackenzie, 1976) have led to the proposal that failure will occur when the void volume fraction reaches a critical level. A point of view which appears feasible for the dynamic case when metallurgical observations are made on specimens which have failed under high strain-rate conditions.

As described earlier, when the quasi-static analysis is carried out to the point where instability occurs, the corresponding value of f at this point is designated as the critical void volume fraction, f_{cr} . The dynamic analysis is then carried out for the strain-rate level of interest, until f reaches the value of f_{cr} . The corresponding uniform strain at this point, ε_{cr}^d , is considered to be the uniform strain at failure, on

the assumption that f_{cr} is independent of the strain-rate of the process.

This procedure is illustrated in Fig. 8, where the void volume fraction is plotted against the uniform strain. The point A in the zero strain-rate case is the point of plastic instability, $d\epsilon^u/d\epsilon^l \rightarrow \infty$. From the numerical solution it was also observed that ϵ_{cr}^d approaches a limiting condition, and did not increase significantly for strain-rates greater than $\dot{\epsilon}_0 = 5000$ 1/sec.

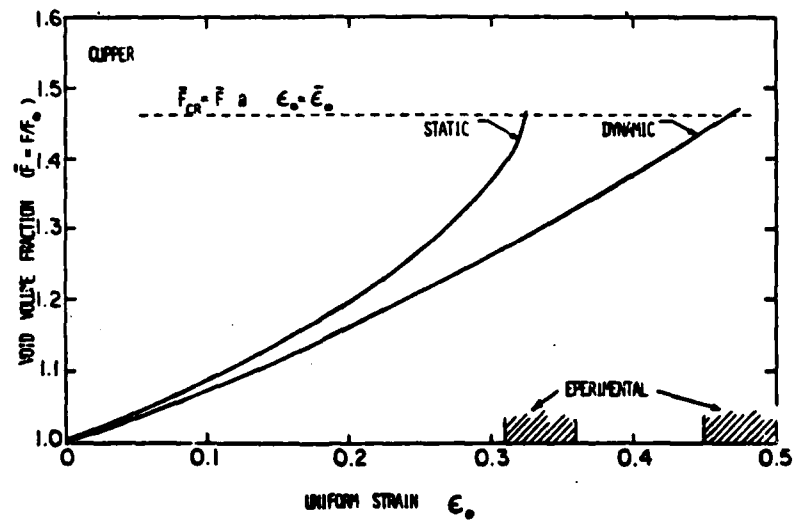
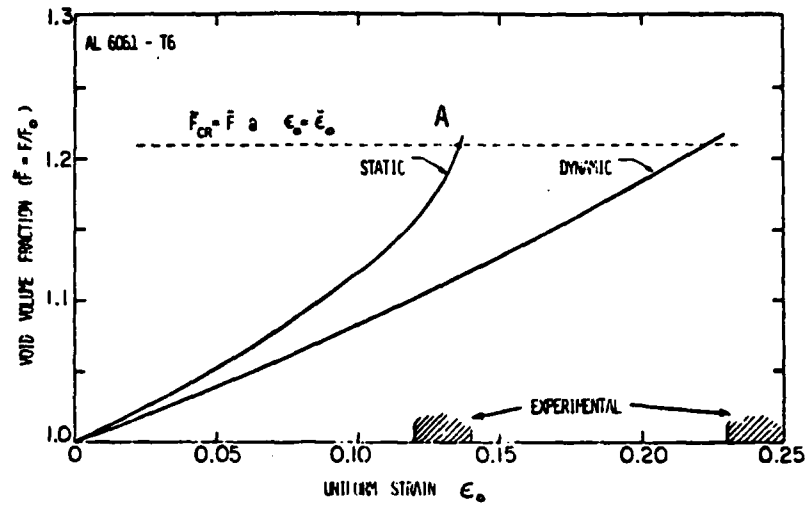


Fig. 8 Critical Void Volume Criterion Applied to Thin Rings of Aluminum and Copper. ($n = 0.03$, $\Delta f = 0.01$).

4. EXPERIMENTAL VERIFICATION

The increase in ductility which occurs in the high strain-rate loading regime has been observed experimentally by the authors in a series of experiments conducted with impulsively loaded thin cylinders. These experiments were adapted to the thin ring configuration, with the objective of determining the uniform strain at failure for both high strain-rate loading and quasi-static loading.

4.1 Dynamic Tests

In the dynamic experiments an exploding wire system was used to generate a symmetric and axially-uniform pressure pulse which propagates radially through the medium surrounding the wire to impinge uniformly on the inner surface of the specimen. This system has the advantage over explosive techniques in that the axial variation caused by the finite detonation velocity is eliminated, and the rings expand without variation in the pressure across their width. The basic test configuration is shown in Fig. 9, in which the wire to be exploded is imbedded in a polyethylene cylinder. The outer diameter of this cylinder was such that the ring specimen could be lightly held in the position shown. The length of the cylinder was not particularly critical, and a length was chosen which produced high strain-rate levels with a uniform displacement of the ring across its width. The general specimen configuration was a ring whose internal diameter was 25.4 mm, width 3 mm and different thicknesses varying in value from 0.5 mm to 1.0 mm. The polyethylene cylinder was approximately 5 cm in length with the 10 cm long wire loosely imbedded in the center.

The above assembly was then attached between the high voltage and

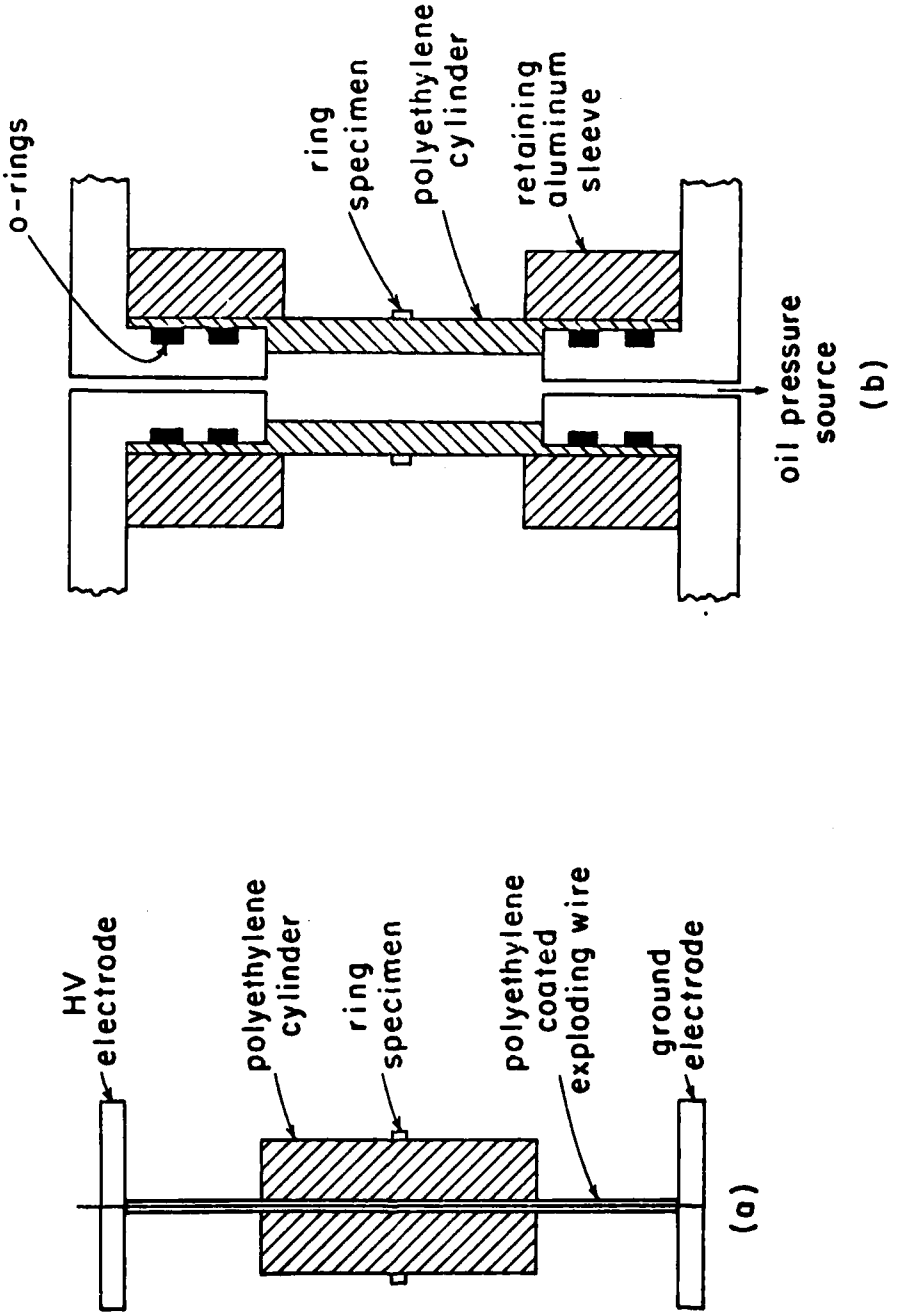


Fig. 9 Specimen Configuration: dynamic (a), static (b).

ground terminals of the capacitor bank system. The capacitor bank system consisted of two or more 15 microfarad capacitors each charged to 20 kilovolts to provide the energy storage of 3,000 joules per capacitor. These capacitors were mechanically switched to discharge through the 10 cm long copper wire. To reduce ringing in the system the diameter of the wire was fixed at 0.84 mm., and the resultant pressure pulse was approximately 5 μ secs in duration.

In order to obtain the input conditions appropriate to the theoretical analysis in sections 2 and 3 it was necessary to obtain the strain rate of the uniform section of the ring. The hoop strain rate ($\dot{\epsilon}_\theta^H$) was determined by optical techniques to eliminate the magnetic interference associated with exploding wire systems. The system found to be most successful is one which measures the light variation of a small collimated beam passing between the ring and a fixed knife edge positioned perpendicular to the specimen. The light intensity variation is detected by a photomultiplier tube, located beyond the test section area I_{rs} output is amplified, and displayed on an oscilloscope.

In Figure 10 a schematic diagram of this system is shown. A small gas laser (Spectra Physics 122) provides the required intense parallel beam of light. This beam was expanded by a suitable lens system to allow the beam to fill the gap between ring and knife-edge. By careful adjustment of the lenses it was possible to obtain a photomultiplier output which varied linearly with the ring displacement. The light beam is contained by a rigid plastic conduit, located a few centimeters past the specimen. The front of the tube is sealed except for a small slit slightly larger than the gap at the specimen, and a lens to reduce the laser beam

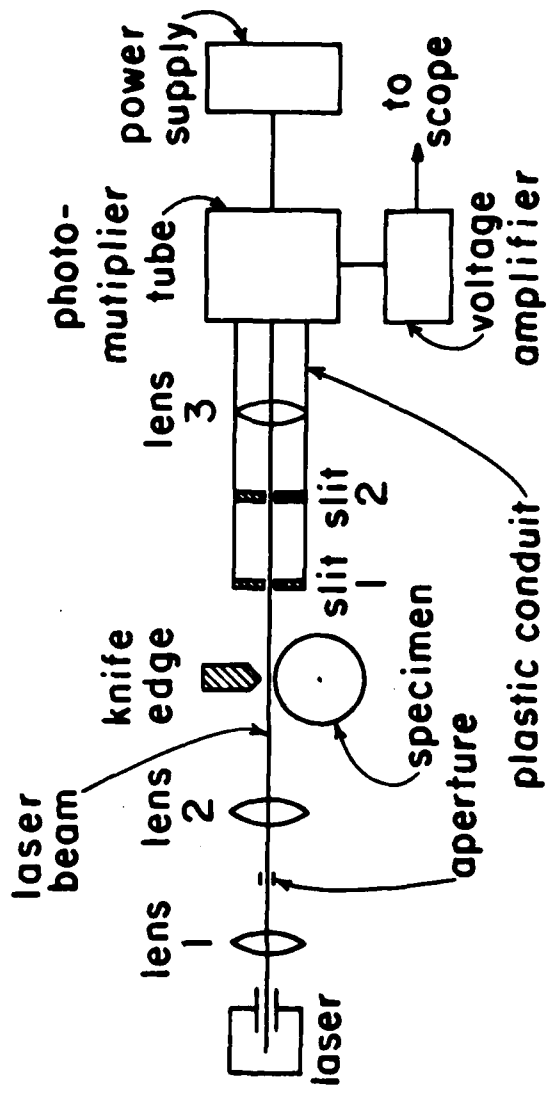


Fig. 10 Schematic of Photomultiplier Strain-Rate Detector

is placed at the photomultiplier end. In between this slit and the lens, another slit was introduced and this further removed any irregularities in the diverging laser beam passing through the first slit. A RCA 4459 photomultiplier tube is employed and its output signal amplified by a voltage amplifier to provide the signal to the oscilloscope. A Hewlett Packard 6513A D.C. regulated power supply supplies power to the P.M. tube. The bandwidth of the amplifier is from 60 hertz to 20 megahertz with a gain of 82.

The calibration technique simulates the motion of the specimen under dynamic loading. The specimen placed in the holder is allowed to slide horizontally toward the knife edge on a "V" guide. Control of this movement is accomplished by using a micrometer with a minimum direct readout of 0.0001 inch. The knife is aligned vertically parallel to the specimen surface. As the specimen is moved toward the knife edge in prescribed increments, the variation of the output of the P.M. tube is monitored by a digital voltmeter. This provides a displacement-voltage calibration. The specimen holder is then restrained at the maximum gap selected for the test, and the shot fired, giving a recorded voltage-time history of the ring expansion.

The above calibration technique is not particularly accurate when used with thin ring specimens. Two sources of error are possible. One is related to using the rigid body displacement of the ring rather than its expansion, while the other is related to a different light level passing through the slit if the ring expands away from the polyethylene cylinder. These errors could well be considerable if accurate strain-rate levels were required during the total expansion of the ring. However, as can be

seen in Fig. 3, the variation in the uniform strain is not greatly effected by the strain-rate level above 1×10^3 1/sec. The initial strain-rate of the ring is not affected by the above errors and this value was used in the calculations described in the previous section. Also the second error would indicate a slower strain-rate level than was actually the case, but the system indicated high strain-rates throughout the whole deformation process. The strain-rates measured by this technique varied with the applied load as controlled by the voltage level of the capacitors.

The pieces from the fractured specimen were trapped in a foam lined box, which also prevented any additional deformation due to their impacting the test fixture.

4.2 Static Tests

The static test apparatus was designed to expand the same configuration of ring specimen as used in the dynamic tests. Again the load was applied indirectly through a polyethylene cylinder, but in this case the cylinder was internally loaded by oil pressure. The test configuration is shown in Fig. 9b. The radial expansion of the ring was measured using a linear voltage differential transformer system, whose actuator rod was displaced by the direct expansion of the ring.

Calibration for this system was obtained by moving the LVDT rod against a micrometer which was adjusted to give a voltage-rod displacement curve. The results of these tests were usually recorded on an x-y plotter in which internal pressure as a function of ring displacement was recorded. However, in this case the pressure had no significance, and no

attempt was made to find the stress level in the ring. The hoop strain was obtained directly from Equation (2.1).

4.3 Experimental Results

In the static tests, the uniform hoop strain at failure could be obtained quite readily, but in the dynamic tests it was not possible to determine this value directly from the change in diameter of the ring. However, assuming that the uniform section of the ring always remained plastically incompressible, ϵ_θ could be obtained from ϵ_z as in Equation (2.2) where ϵ_z was the measure of the change in width of the ring.

A series of experiments were carried out in which the ring was expanded to a diameter just short of failure. Comparing the ϵ_θ obtained from the change in diameter and from the change in the width, it was found that these results were quite compatible with the incompressibility assumption and the scatter was within three percent strain. From incompressibility it would also have been possible to use ϵ_r from the changes in thickness. However, the scatter in this case was such that a reliable reading of ϵ_θ could not be obtained. This result was inherent in the thin ring configuration, where an error of 0.0006 in. in the thickness measurement resulted in a six to seven percent strain variation in the hoop strain value. Although compressibility in the uniform section could not be accurately confirmed by these measurements the results were not incompatible with this assumption.

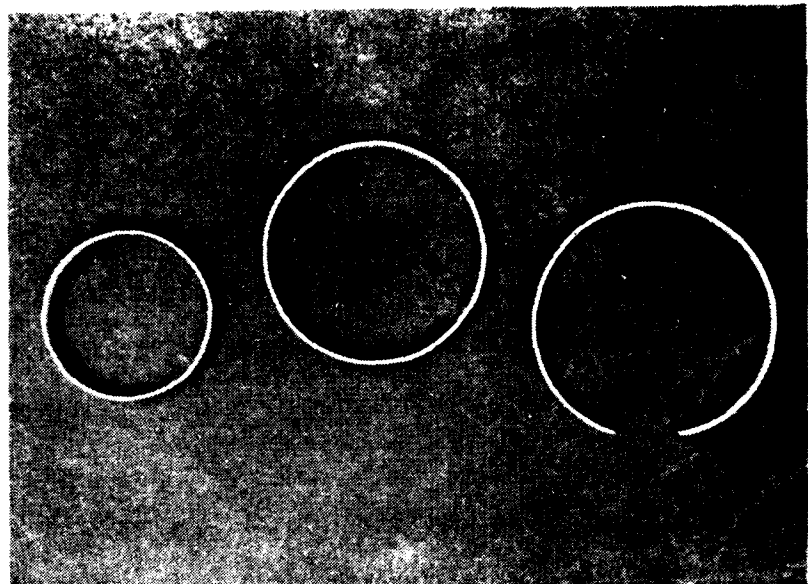
With the dynamic tests conducted at various voltage levels of the capaciter bank, and thus different strain rate levels, the number of pieces into which the ring broke varied. As was to be expected the lower

the strain-rate of loading the fewer failure points occurred in the specimen. At the highest strain-rate levels as many as ten failure points were observed. With the hoop strain values being obtained from the width of a uniform section of the broken ring it was found that a uniform section, free from necking, could be expected when the strain-rate level produced about five failure points. This level of strain rate was sufficiently high that the additional strain due to inertia amounted to approximately 85% for 6061-T6 aluminum and about 45% for copper. These results are presented in Fig. 8 and are fairly typical of the results obtained from similar tests carried out on thin cylinders of the same materials. In tests where nine or ten failure points did occur, but in which at least one portion of the fractured ring was large enough to allow the calculation of the hoop strain, it was observed that the strain at failure had not increased significantly over those values obtained with about five failure points. This result is compatible with the theoretical prediction that the strain at failure approaches the limiting curve $\epsilon_{\theta}^U = \epsilon_{\theta}^L$ of Fig. 1, and suggests that failure could occur at a constant level of ϵ_{θ}^L or at a critical void volume fraction which is essentially strain-rate independent. It was results such as these that suggested the use of the critical void volume fraction criterion proposed in Section 3.3.

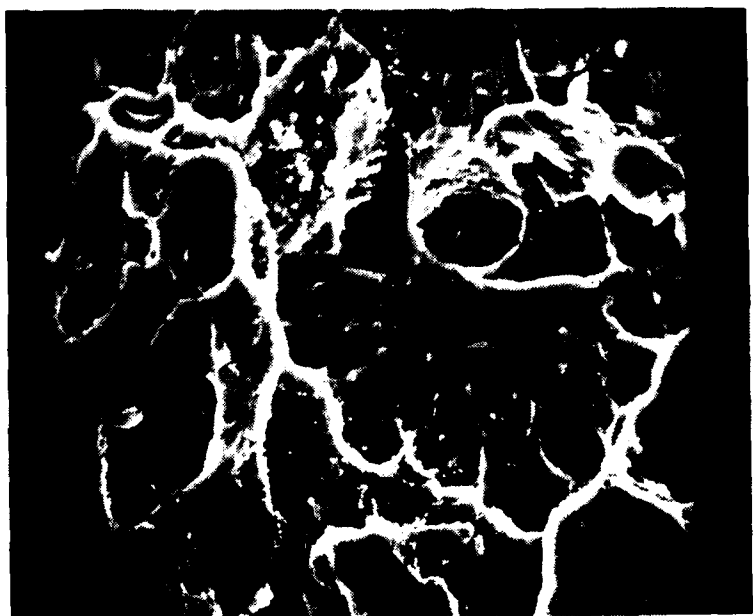
The uniform strain at failure is very sensitive to the two parameters which define the geometric and metallurgical imprecisions, n and Δf . Although n can be found by a careful measurement of the ring specimen, the problem of determining an accurate value of n is directly related to the thickness of the ring, which for thin rings results in a value of n

that is at best only a reasonable approximation. The value of Δf on the other hand is only an educated guess, and the value chosen for this study was one used by Needleman and Triantafyllidis (1978) which, although probably unrealistically high, is felt to be compatible with the simplified constitutive model used in the study. So, it may be possible to pick different combinations of n and Δf which would allow the theory to predict a value of ϵ_0^f in agreement with the quasi-static test results in Fig. 8. However, that these same values also accurately predict the dynamic test values for the two materials is encouraging. Since the dimensions of the ring specimens for both the Al. 6061-T6 and the annealed copper are identical, the value of n was naturally the same in both cases, and the same value of Δf was considered to be appropriate lacking any evidence to the contrary.

Fig. 11 shows the symmetry of the ring expansion under dynamic loading conditions, and the metallographic evidence of void growth ductile fracture at the failure cross-section.



(a)



(b)

Fig. 11 Expanded Ring Specimens (a), Typical SEM of Fracture Surface (b).

5. CONCLUSIONS

The use of a constitutive model, which allows for plastic compressibility in the region of either a metallurgical or geometric flaw, although somewhat complex, provides results which appear to be compatible with the more traditional treatment of necking instability. The concept of a critical void volume level as a means to predict failure is a natural outgrowth of the use of this model, and encouraging results were obtained in its application to thin rings undergoing both static and dynamic expansion.

For a material which is perfectly plastic the incompressible model predicts the strain at failure to occur at the onset of plastic flow. The compressible model, however, in addition to providing a failure criterion applicable for conditions where inertia is important, also gives a more realistic failure strain for materials of this kind. This particular feature of the compressible model may be due in part to assumption of a perfectly plastic matrix material. It thus also might be expected that less meaningful results would occur for high strain hardening materials. In the present model the strain hardening effect is introduced, rather artificially, through the tangent modulus E_t . However, in comparing the results of this analysis in its application to the aluminum and copper rings it is interesting to note that the theory predicts not only the large ductility expected of the copper, but also the reduced effect of inertia in this material in contrast to the aluminum; a result which is clearly seen in Fig. 8.

The problem of determining meaningful values for the non-uniformity parameter η is essentially more a function of the specimen geometry, and so reasonable values can usually be obtained. Unfortunately, this is not the case for Δf . In principle, this value should be obtainable from metallurgical experiments, but even if values were available, it is unlikely that they would be compatible with the requirements imposed by the approximate void growth model used. From the point of view of dynamic failure prediction, at present, it appears sufficient to use the values necessary to obtain the failure strain in the static tests.

The analysis presented in this study was designed to predict the strain at the onset of ductile fracture, and no consideration has been given to void nucleation or the particular mode of failure which might ensue beyond this strain level. It is to be expected that this latter aspect of the failure process can only be determined from a more detailed analysis of the stress field in the necking region.

The extension of the approach outlined in this study to different geometric configurations, in which the role of the non-uniformity parameter η can be neglected is a necessary step to further the efforts to incorporate microstructural features in the analyses of ductile fracture.

REFERENCES

- 1.) Argon, A. S., Im, J., and Safoglu, R., "Cavity Formation from Inclusions in Ductile Fracture", Metallurgical Transactions A., Vol. 6A, 1975, p. 825.
- 2.) Beachem, C. D., "An Electron Fractographic Study of the Influence of Plastic Strain Conditions Upon Ductile Rupture Processes in Metals", Transactions of the A.S.M., Vol. 56, 1963, p. 318.
- 3.) Berg, C. A., "Plastic Dilation and Void Interaction" in the Proc. of the Batelle Memorial Institute Symposium on Inelastic Processes in Solids, 1969, p. 171.
- 4.) Campbell, J. D., "Plastic Instability in Rate Dependent Materials", J. of the Mechanics and Physics of Solids, Vol. 15, 1967, p. 359.
- 5.) Campbell, J. D., Eleiche, A.M. and Tsao, M.C.C., Fundamental Aspects of Structural Alloy Design, (Edited by Jafee, R. J.), p. 545, Plenum Press, New York, 1977.
- 6.) Considére, A., Ann. Ponts Chausées 9, p. 574 (1885).
- 7.) Darlington, H., "Ductile Fracture Under Axisymmetric Stresses in Electrolytic Iron and Spheroidized Low-Carbon Steel", Ph.D. Diss. Dept. of Metallurgy and Materials Science, Lehigh University, Bethlehem, Pa., 1971.
- 8.) Demeri, M. Y., and Conrad, H., "Instability of Plastic Flow in Tension", Scripta Metallurgica, Vol. 12, p. 389, May, 1978.
- 9.) Deutler, H., "Experimentelle Untersuchen Ueber die Abhaengigkeit, der Zugspannungen Von Verformungsgeschwindigkeit," Physicalische Zeitschrift, Vol. 33, 1932, p. 247.

- 10.) Fyfe, I. M. and Rajendran, A. M., "Dynamic Pre-Strain and Inertia Effects on the Fracture of Metals", *J. of the Mechanics and Physics of Solids*, Vol. 28, 1980.
- 11.) Ghosh, A. K., "Tensile Instability and Necking in Materials with Strain Hardening and Strain-rate Hardening", *Acta Metallurgica*, Vol. 25, 1977a, p. 1413.
- 12.) Ghosh, A. K., "The Influence of Strain Hardening and Strain-rate Sensitivity on Sheet Metal Forming", *J. of Engineering Materials and Technology*, *Trans. of the ASME*, p. 264, July 1977b.
- 13.) Gurland, J. and Plateau, J., "The Mechanism of Ductile Rupture of Metals Containing Inclusions," *Transactions of the A.S.M.E.*, Vol. 56, 1963, p. 443.
- 14.) Gurson, A. L., "Plastic Flow and Fracture Behavior of Ductile Materials Incorporating Void Nucleation, Growth and Interaction," *Ph.D. Dissertation*, Brown University, 1975.
- 15.) Hancock, J. W. and Mackenzie, A. C., "On the Mechanisms of Ductile Rupture in High-Strength Steels Subjected to Multi-axial Stress-states", *J. of the Mechanics and Physics of Solids*, Vol. 24, 1976, p. 147.
- 16.) Hart, E. W., "Theory of Tensile Test", *Acta Metallurgica*, Vol. 15, p. 351, Feb. 1967.
- 17.) Hutchinson, J. W. and Neale, K. W., "Influence of Strain-rate Sensitivity on Necking Under Uniaxial Tension", *Acta Metallurgica*, Vol. 25, 1977, p. 839.
- 18.) Jonas, J. J., and Christodoulou, N., "The Onset of Plastic Instability in Tensile Samples Containing Deformation Defects", *Scripta Metallurgica*, Vol. 12, p. 393, 1978.

- 19.) Malvern, L. E., "The Propagation of Longitudinal Waves of Plastic Deformation in a Bar of Material Exhibiting a Strain-Rate Effect", J. of Applied Mechanics, Trans. ASME, Vol. 18, p. 203, 1951.
- 20.) Marciniak, A. and Kuczynski, K., "Limit Strains in the Process of Stretch Forming Sheet-Metal", Intn. J. of the Mechanical Sciences, Vol. 9, 1967, p. 609.
- 21.) Marciniak, A., Kuczynski, K., and Pokora, T., "Influence of the Plastic Properties of a Material on the Forming Limit Diagram for Sheet Metal in Tension", Intn. J. of the Mechanical Sciences, Vol. 15, 1973, p. 789.
- 22.) McClintock, F. A., "A Criterion for Ductile Fracture by the Growth of Holes", J. of Applied Mechanics, Vol. 35, 1968, p. 363.
- 23.) Nagpal, V., McClintock, F. A., Berg, C. A., and Subudhi, M., "Traction-Displacement Boundary Conditions for Plastic Fracture by Hole Growth", in the Int'l. Symposium on Foundations of Plasticity, Vol. 1, (A. Sawczuk, Ed.), 1972, p. 365.
- 24.) Needleman, A., and Triantafyllidis, N., "Void Growth and Local Necking in Biaxially Stretched Sheets", J. of Engineering Materials and Technology, Trans. of the A.S.M., Vol. 100, April 1978, p. 164.
- 25.) Perzyna, P., "Fundamental Problems in Viscoplasticity", Advances in Applied Mechanics, Academic Press, New York, Vol. 9, 1966.
- 26.) Rice, J. R., and Tracey, D. M., "On the Ductile Enlargements of Voids in Triaxial Stress Fields", J. of the Mechanics and Physics of Solids, Vol. 17, 1969, p. 201.

- 27.) Sagat, S. and Taplin, D. M. R., "The Stability of Plastic Flow in Strain-rate Sensitivity Materials", Metal Science, Vol. 10, 1976, P. 94.
- 28.) Seaman, L., Barbee Jr., T. W. and Curran, D. R., "Dynamic Fracture Criteria of Homogeneous Materials", Technical Report No. AFWL-TR-71-156, 1971 (December) Stanford Research Institute.
- 29.) Wilson, F. W., "High Velocity Forming of Metals", The American Society of Tool and Manufacturer Engineers, New York, 1964.
- 30.) Yamamoto, H., "Conditions for Shear Localization in the Ductile Fracture of Void Containing Materials", Brown University Report D(11-1), p. 3084, Apr. 1977.

UNCLASSIFIED

SECURITY CLASSIFICATION OF THIS PAGE (When Data Entered)

REPORT DOCUMENTATION PAGE		READ INSTRUCTIONS BEFORE COMPLETING FORM
1. REPORT NUMBER DAAG 29-77-G-0211	2. GOVT ACCESSION NO. <i>AD-A088 515</i>	3. RECIPIENT'S CATALOG NUMBER
4. TITLE (and Subtitle) A Void Growth Failure Criterion Applied to Dynamically and Statically Loaded Thin Rings	5. TYPE OF REPORT & PERIOD COVERED	
7. AUTHOR(s) A. M. Rajendran and I. M. Fyfe	6. PERFORMING ORG. REPORT NUMBER 80-10	
9. PERFORMING ORGANIZATION NAME AND ADDRESS Department of Aeronautics and Astronautics University of Washington Seattle, Washington 98195	10. PROGRAM ELEMENT, PROJECT, TASK AREA & WORK UNIT NUMBERS	
11. CONTROLLING OFFICE NAME AND ADDRESS U. S. Army Research Office Post Office Box 12211 Research Triangle Park, NC 27709	12. REPORT DATE June 1980	
14. MONITORING AGENCY NAME & ADDRESS (if different from Controlling Office) NA	13. NUMBER OF PAGES 47	
16. DISTRIBUTION STATEMENT (of this Report) Approved for public release; distribution unlimited.	15. SECURITY CLASS. (of this report) Unclassified	
17. DISTRIBUTION STATEMENT (of the abstract entered in Block 20, if different from Report) NA	15a. DECLASSIFICATION/DOWNGRADING SCHEDULE NA	
18. SUPPLEMENTARY NOTES The findings in this report are not to be construed as an official Department of the Army position, unless so designated by other authorized documents.		
19. KEY WORDS (Continue on reverse side if necessary and identify by block number) Dynamic Fracture Ductile Fracture Thin Rings Plastic Instability Void Growth		
20. ABSTRACT (Continue on reverse side if necessary and identify by block number) The introduction of inertia terms in the theoretical model of thin ring expansion shows that classical plastic instability concepts, defined in terms of the local strain in the necking region, no longer apply. However, in this report it is shown that, when the plastically incompressible constitutive model is replaced with a model applicable to porous plastic materials, a criterion based on critical void volume fraction provides an alternative means to predict failure. The theory also provides a method in which both geometric and metallurgical imperfections in a given sample might be considered. (over)		

UNCLASSIFIED

SECURITY CLASSIFICATION OF THIS PAGE(When Data Entered)

20. Abstract (Continued)

The application of this theory to thin ring specimens was used to confirm that the critical void growth concept predicts the uniform strain at failure as observed in aluminum and copper rings, under both quasi-static and high strain-rate loading conditions.

UNCLASSIFIED

SECURITY CLASSIFICATION OF THIS PAGE(When Data Entered)